

## TURBULENCE AND ANGULAR MOMENTUM TRANSPORT IN A GLOBAL ACCRETION DISK SIMULATION

PHILIP J. ARMITAGE

Canadian Institute for Theoretical Astrophysics, McLennan Labs, 60 St George St, Toronto, M5S 3H8,  
Canada

*ApJ Letters, in press*

### ABSTRACT

The global development of magnetohydrodynamic turbulence in an accretion disk is studied within a simplified disk model that omits vertical stratification. Starting with a weak vertical seed field, a saturated state is obtained after a few tens of orbits in which the energy in the predominantly toroidal magnetic field is still subthermal. The efficiency of angular momentum transport, parameterized by the Shakura-Sunyaev  $\alpha$  parameter, is of the order of  $10^{-1}$ . The dominant contribution to  $\alpha$  comes from magnetic stresses, which are enhanced by the presence of weak net vertical fields. The power spectra of the magnetic fields are flat or decline only slowly towards the largest scales accessible in the calculation, suggesting that the viscosity arising from MHD turbulence may not be a locally determined quantity. I discuss how these results compare with observationally inferred values of  $\alpha$ , and possible implications for models of jet formation.

*Subject headings:* accretion, accretion disks — hydrodynamics — instabilities — magnetic fields — MHD — turbulence

*For visualization of simulations see [http://www.cita.utoronto.ca/~armitage/global\\_abs.html](http://www.cita.utoronto.ca/~armitage/global_abs.html)*

### 1. INTRODUCTION

The Balbus-Hawley instability is the most generally applicable mechanism known to initiate turbulence and outward angular momentum transport in accretion disks (Balbus & Hawley 1991). This is a linear, local instability that exists for rotating flows threaded by a weak magnetic field with  $d\Omega^2/dr < 0$ , conditions satisfied in disks (for earlier discussions see Velikhov 1959, Chandrasekhar 1961). A vigorous growth rate is obtained for a wide variety of initial magnetic field configurations (Balbus & Hawley 1992; Ogilvie & Pringle 1996; Terquem & Papaloizou 1996), implying that the instability is inescapable for ionized disks where the field is well-coupled to the gas.

Extensive numerical simulations have explored the nonlinear development of the instability within the local, shearing box approximation (for a review, see e.g. Gammie 1998). Such simulations have convincingly established that the nonlinear development of the Balbus-Hawley instability leads to sustained turbulence and significant angular momentum transport, typically finding a Shakura-Sunyaev (1973)  $\alpha \approx 10^{-2}$  (Hawley, Gammie & Balbus 1995, 1996; Stone et al 1996; Brandenburg et al. 1995). There is some evidence for cyclic behavior that might have important implications for disk variability (Brandenburg et al. 1996). Equally important has been the final elimination of convection (Stone & Balbus 1996), and the near-elimination of nonlinear hydrodynamic turbulence (Balbus, Hawley & Stone 1996), as plausible rival mechanisms for angular momentum transport in accretion disks. Progress has also been made in trying to understand how the rich phenomenology of accretion disk variability can arise within a dynamo driven disk model (Armitage, Livio & Pringle 1996; Gammie & Menou 1998), although much more remains to be done in this area.

There are many further questions that one may hope simulations will address, and not all of them are amenable

to a local treatment. Most obviously, is the angular momentum transport in a disk locally determined? What is the structure of the spatial and time variability of the disk fields, and are they suitable for launching a magnetically driven disk wind or jet? Unsurprisingly, the global calculations needed to investigate these issues are extremely demanding, both as a consequence of the larger computational domain and, especially, because of the need to simulate regions of low density where the high Alfvén speed severely limits the timestep of explicit numerical codes.

In this paper, results are presented from a vertically unstratified global simulation of accretion disk turbulence. Such a calculation is evidently missing essential physics. There is no buoyancy, no possibility of Parker instability (Parker 1979), and no magnetically dominated disk corona – all features that are expected to arise in a full disk model and which may be crucial for the disk dynamo problem (Tout & Pringle 1992). However the lesser computational demands permit a preliminary investigation of some of the important questions raised by previous, local, simulations.

### 2. NUMERICAL SIMULATION

The equations of ideal magnetohydrodynamics (MHD) are solved using the ZEUS-3D code developed by the Laboratory for Computational Astrophysics (Clarke, Norman & Fiedler 1994; Stone & Norman 1992a, 1992b). ZEUS is a time explicit eulerian finite difference code that uses the method of characteristics (MoC) – constrained transport scheme to evolve the magnetic fields (Hawley & Stone 1995; Stone & Norman 1992b). For this simulation an isothermal equation of state  $P = \rho c_s^2$  replaces the internal energy equation, so the remaining equations are:

$$\frac{\partial \rho}{\partial t} + \nabla \cdot (\rho \vec{v}) = 0 \quad (1)$$

$$\frac{\partial (\rho \vec{v})}{\partial t} + \nabla \cdot (\rho \vec{v} \vec{v}) = -\nabla P - \rho \nabla \Phi + \vec{J} \times \vec{B} \quad (2)$$

$$\frac{\partial \vec{B}}{\partial t} = \nabla \times (\vec{v} \times \vec{B}), \quad (3)$$

where the symbols have their conventional meanings. There is no explicit resistivity in the calculation, reconnection occurs numerically on the grid scale. We use second order interpolation (van Leer 1977) for all advected quantities, and the latest (and allegedly most stable) version of the MoC algorithm for the induction equation.

### 2.1. Initial and boundary conditions

The calculation is performed in cylindrical polar geometry  $(r, \phi, z)$ , in a volume bounded by  $r_{\text{in}} = 1$ ,  $r_{\text{out}} = 4$ , and  $z = \pm H = 0.4$ . We take  $\Phi = \Phi(r) = 1/r$ , implying no vertical component of gravity. The boundary conditions are periodic in  $z$ , reflecting at  $r = r_{\text{in}}$  ( $v_r = B_r = 0$ ), and set to outflow at  $r = r_{\text{out}}$ . Outflow boundary conditions are implemented as a simple extrapolation of fluid variables on the grid into the boundary zones. These boundary conditions admit the development of net vertical flux through the computational volume as material leaves the grid – the import of this for the resulting  $\alpha$  will be discussed later. We use a grid of ( $n_r = 128, n_\phi = 320, n_z = 32$ ) zones, with uniform zoning.

An initial state is obtained by evolving a disk with constant surface density and Keplerian rotation in two dimensions until transients due to pressure gradients and the influence of the inner boundary condition die out. This requires a time  $\Delta t = 100$ , where time is measured in units of the orbital period at the inner edge. The resulting equilibrium state has  $\Sigma = \text{constant}$  between  $R = 1.4$  and  $R = 3$ , tapering to a low value at the boundaries. The velocity profile is Keplerian to better than 10% over the entire radial range. No evidence is found for purely hydrodynamic disk instabilities. We then add a weak vertical magnetic field that is non-zero only between  $r = 1.5$  and  $r = 3.5$ , of the form,

$$B_z(r) = \frac{B_0}{r} \sin(\pi(r - 1.5)), \quad (4)$$

chosen simply to be divergence free and to have zero net flux in the  $z$  direction. The simulation is then evolved for a further 80 orbits. The computational cost of this using ZEUS is approximately  $2 \times 10^{14}$  floating point operations – a large but not outrageous number for current workstations.

### 2.2. Results

The initial state is immediately unstable, leading to rapid growth in the magnetic and perturbed velocity fields. Around 40 inner orbits of evolution were required before a saturated state was obtained, which was then followed for an additional time  $\Delta t = 40$  without any further qualitative changes in disk behavior occurring. The magnetic energy in the saturated state is dominated by the toroidal field component and is subthermal,  $\sim 0.2 - 0.3$  of the thermal energy, the corresponding energies in  $B_r$  and  $B_z$  are respectively  $10^{-2}$  and  $6 \times 10^{-3}$  of the thermal energy. The velocity perturbations are mildly anisotropic,  $v_z$  and  $\delta v_\phi$  display roughly gaussian distributions with width  $\approx 0.3c_s$ , while that of  $v_r$  has a width of  $\approx 0.4 - 0.5c_s$ . The total energy in the perturbed velocity field is an order of magnitude below that of the magnetic fields.

Fig. 1 shows the surface density and vertically averaged  $B_z$  component of the magnetic field at the conclusion of the calculation. We plot the overdensity  $\delta\Sigma$  relative to the azimuthally averaged surface density profile,

$$\delta\Sigma(r, \phi) = \frac{2\pi\Sigma(r, \phi)}{\int_0^{2\pi} \Sigma(r, \phi) d\phi}. \quad (5)$$

The magnetic field is plotted without any such normalization.

The combination of turbulence and shear leads to a ragged spiral pattern in the surface density, though the azimuthal fluctuations are relatively small and described by a gaussian with a width  $\sim 0.35\Sigma(r)$ . The magnetic field displays a filamentary structure, both in projection and when visualized in three dimensions. Visually it is evident that the field shows considerable coherence over large scales, especially in azimuth.  $B_r$  and  $B_\phi$  (not plotted) show similar patterns.

### 2.3. Efficiency of angular momentum transport

The efficiency of angular momentum transport in the simulation can be measured by  $\alpha$ , the ratio of the shear stress  $w_{r\phi}$  to the gas pressure  $P$  in the form,

$$\alpha = \frac{2}{3} \frac{w_{r\phi}}{P}. \quad (6)$$

This is consistent with a relation between the shear viscosity  $\nu$  and the disk sound speed  $c_s$  of the usual form,  $\nu = \alpha c_s^2 / \Omega$ , with  $\Omega$  the Keplerian angular velocity. The magnetic and fluid contributions to the total stress are then given by (e.g. Gammie 1998),

$$\alpha_M = \frac{2}{3} \left\langle \frac{-B_r B_\phi}{4\pi P} \right\rangle, \quad \alpha_R = \frac{2}{3} \left\langle \frac{\rho v_r \delta v_\phi}{P} \right\rangle, \quad (7)$$

respectively, where the brackets denote an average in the spatial co-ordinates.

Fig. 2 shows the time evolution of  $\alpha_M$  and  $\alpha_R$  at a single radius  $r = 0.5(r_{\text{in}} + r_{\text{out}})$  in the disk. Apart from some transient waves at early times,  $\alpha$  from both fluid and magnetic stresses is positive, with the bulk of the angular momentum transport being provided by magnetic stresses. At the end of the calculation, the total  $\alpha$  at this radial location is in the range  $\alpha = 0.05 - 0.1$ .

Evaluating  $\alpha_M$  and  $\alpha_R$  as functions of radius at  $t = 80$ ,  $\alpha_R$  is found to be roughly constant across the grid in the range  $\alpha_R = 0.01 - 0.02$ .  $\alpha_M$  varies by factors of a few, and is close to its minimum value at the location in the center of the grid used for plotting the time series in Fig. 2. Taking an average over the entire simulation volume, we obtain,

$$\alpha_M \simeq 0.17, \quad \alpha_R \simeq 2.0 \times 10^{-2}. \quad (8)$$

The value of  $\alpha$  can also be estimated by comparing the simulation to the results of one dimensional diffusive disk models (e.g. Pringle 1981). Comparing the evolution of the radial center of mass between the two calculations one again obtains an  $\alpha$  value of  $\sim 0.1$ , though as mentioned already  $\alpha$  is unsurprisingly not a constant in the simulation.

#### 2.4. Influence of net vertical magnetic field

The choice of outflow boundary conditions at  $r_{\text{out}}$  was motivated by the desire to reduce the amplitude of reflected waves at the edge of the grid. However these boundary conditions also allow the development of net vertical magnetic fields that can have a strong influence on the properties of disk turbulence. Previous work has found that a net field significantly enhances the strength of turbulence and boosts the derived value of  $\alpha$  (Hawley, Gammie & Balbus 1995). Adopting the parameterization of the results of local simulations given by Gammie (1998),

$$\alpha \sim 0.01 + 4 \frac{\langle v_{Az} \rangle}{c_s} + \frac{1}{4} \frac{\langle v_{A\phi} \rangle}{c_s}, \quad (9)$$

where  $v_{Az}$  is the Alfvén velocity corresponding to the net vertical field, we find that the enhancement of  $\alpha$  in this simulation due to net fields is expected to be  $\sim 0.05$ . This is obviously a very crude estimate, as we are using the above relation in an untested regime, but it does imply that it is premature to conclude that global simulations lead to higher values of  $\alpha$  than local calculations.

#### 2.5. Coherence of the magnetic field

The scale of the magnetic fields generated in the disk is analyzed via the azimuthal Fourier decomposition,

$$C_{m,i}(r, z) = \frac{1}{2\pi} \int_0^{2\pi} B_i e^{-im\phi} d\phi. \quad (10)$$

Fig. 3 plots  $m|C_m|^2$  for the three field components, in each case averaged over the entire volume of the simulation.

The azimuthal power spectra show similar shapes for each of the magnetic field components. There is a power-law decline somewhat steeper than that expected from Kolmogorov turbulence at large  $m$ , and a break at  $m \simeq 10 - 20$ , corresponding to a physical scale of  $\sim H$  in the center of the grid. This confirms the visual impression that the magnetic fields are patchy with typical scales of the order of  $H$ . However there is also considerable power at the largest scales, with the power per logarithmic interval in  $m$  declining only slowly towards low  $m$  for all field components in the range  $m = 1 - 10$ . Similar conclusions follow from the radial power spectra.

### 3. DISCUSSION

In this paper, we have reported on a global simulation of an unstratified magnetized accretion disk. As expected from analytic considerations (Curry & Pudritz 1994, 1995, 1996) and local simulations, MHD instabilities generate sustained turbulence that leads to outward transport of angular momentum. The generated fields possess considerable power in azimuthal modes of low  $m$ , which correspond to physical scales considerably in excess of  $H$ , the disk semi-thickness, and display a ragged spiral structure. The current simulation does not admit the development of the Parker instability, which might depress the power on large scales, but with this caveat the results suggest that a viscosity originating from MHD turbulence may not be a locally determined quantity. The dominant magnetic field component is toroidal, and the interaction of this fluctuating internal field with a magnetosphere is likely to be an

important complication to the already complex picture of star-disk interaction in magnetic systems (Miller & Stone 1997; Torkelsson 1998).

The efficiency of angular momentum transport seen in the calculation, parameterized by the Shakura-Sunyaev  $\alpha$  prescription, is  $\alpha \approx 10^{-1}$ . This is larger than the value obtained from local calculations (Gammie 1998) with zero net vertical magnetic fields, though we have noted that the influence of a vertical field on the current simulation is likely to have boosted the value of  $\alpha$  significantly. More realistic simulations with demonstrated numerical convergence are evidently required. However there is no obvious discrepancy with the values of  $\alpha$  inferred for dwarf novae, where modeling of disk outbursts suggests  $\alpha = 0.1 - 0.3$  (Cannizzo 1993), and for Active Galactic Nuclei, where the admittedly poorer observations are consistent with an  $\alpha$  of  $10^{-2}$  (Siemiginowska & Czerny 1989). Conversely it is hard to see why a viscosity derived from MHD turbulence should be two or three orders of magnitude *lower* in the ionized inner regions of protostellar disks, as required to match the timescales of FU Orionis outbursts within disk instability models (Bell & Lin 1994). This may call into question the *self-regulated* aspect of the thermal disk instability picture for FU Orionis events. The generation of magnetic fields of large scale may additionally be important for models of jet formation (eg. Blandford & Payne 1982; Ouyed, Pudritz & Stone 1997; Matsumoto & Shibata 1997; Konigl 1997), which if generated via a disk dynamo would be expected to be most efficient in relatively thick disks or advection dominated flows (Narayan & Yi 1995). Observations of which systems produce jets appear to be broadly consistent with a model in which  $(H/R)$  is a controlling parameter, though many other possibilities are also viable (Livio 1997).

I thank Jim Stone and James Murray for valuable discussions at the start of this work, and the referee for a very prompt and helpful report. I am grateful to Mark Bartelt for ensuring the availability of the required computing resources.

## REFERENCES

- Armitage, P. J., Livio, M., & Pringle, J. E. 1996, *ApJ*, 457, 332
- Balbus, S. A., & Hawley, J. F. 1991, *ApJ*, 376, 214
- Balbus, S. A., & Hawley, J. F., 1992, *ApJ*, 400, 610
- Balbus, S. A., Hawley, J. F., & Stone, J. M. 1996, *ApJ*, 467, 76
- Bell, K. R., & Lin, D. N. C. 1994, *ApJ*, 427, 987
- Blandford, R. D., & Payne, D. G. 1982, *MNRAS*, 199, 883
- Brandenburg, A., Nordlund, A., Stein, R. F., & Torkelsson, U. 1995, *ApJ*, 446, 741
- Brandenburg, A., Nordlund, A., Stein, R. F., & Torkelsson, U. 1996, *ApJ*, 458, L45
- Cannizzo, J. K. 1993, *ApJ*, 419, 318
- Chandrasekhar, S. 1961, in *Hydrodynamic and Hydromagnetic Stability*, Oxford University Press, Oxford, p. 384
- Clarke, D. A., Norman, M. L., & Fiedler, R. A. 1994, National Center for Supercomputing Applications Technical Report 015
- Curry, C., & Pudritz, R. E. 1994, *ApJ*, 434, 206
- Curry, C., & Pudritz, R. E. 1995, *ApJ*, 453, 697
- Curry, C., & Pudritz, R. E. 1996, *MNRAS*, 281, 119
- Gammie, C. F. 1998, in *Accretion Processes in Astrophysical Systems: Some Like It Hot*, eds. S. Holt and T. Kallman, in press
- Gammie, C. F., & Menou, K. 1998, *ApJ*, 492, L75
- Hawley, J. F., Gammie, C. F., & Balbus, S. A. 1995, *ApJ*, 440, 742
- Hawley, J. F., Gammie, C. F., & Balbus, S. A. 1996, *ApJ*, 464, 690
- Konigl, A. 1997, in *Accretion Phenomena and Related Outflows*, eds. D. T. Wickramasinghe, G. V. Bicknell & L. Ferrario, A.S.P. Conf. Ser. volume 121, p. 551
- Livio, M. 1997, in *Accretion Phenomena and Related Outflows*, eds. D. T. Wickramasinghe, G. V. Bicknell & L. Ferrario, A.S.P. Conf. Ser. volume 121, p. 845
- Matsumoto, R., & Shibata, K. 1997, in *Accretion Phenomena and Related Outflows*, eds. D. T. Wickramasinghe, G. V. Bicknell & L. Ferrario, A.S.P. Conf. Ser. volume 121, p. 443
- Miller, K. A., & Stone, J. M. 1997, *ApJ*, 489, 890
- Narayan, R., & Yi, I., 1995, *ApJ*, 444, 231
- Ogilvie, G. I., & Pringle, J. E. 1996, *MNRAS*, 279, 1520
- Ouyed, R., Pudritz, R. E., & Stone, J. M. 1997, *Nature*, 385, 409
- Parker, E. N. 1979, in *Cosmical Magnetic Fields*, Oxford University Press, Oxford, p. 330
- Pringle, J. E. 1981, *ARA&A*, 19, 137
- Shakura, N. I., & Sunyaev, R. A. 1973, *A&A*, 24, 337
- Siemiginowska, A., & Czerny, B. 1989, *MNRAS*, 239, 289
- Stone, J. M., & Balbus, S. A. 1996, *ApJ*, 464, 364
- Stone, J. M., Hawley, J. F., Gammie, C. F., & Balbus, S. A. 1996, *ApJ*, 463, 656
- Stone, J. M., & Norman, M. L. 1992a, *ApJS*, 80, 791
- Stone, J. M., & Norman, M. L. 1992b, *ApJS*, 80, 819
- Terquem, C., & Papaloizou, J. C. B. 1996, *MNRAS*, 279, 767
- Torkelsson, U., 1998, *MNRAS*, submitted
- Tout, C. A., & Pringle, J. E. 1992, *MNRAS*, 259, 604
- van Leer, B. 1977, *J. Comp. Phys.*, 23, 276
- Velikhov, E. P. 1959, *Soviet JETP*, 36, 995

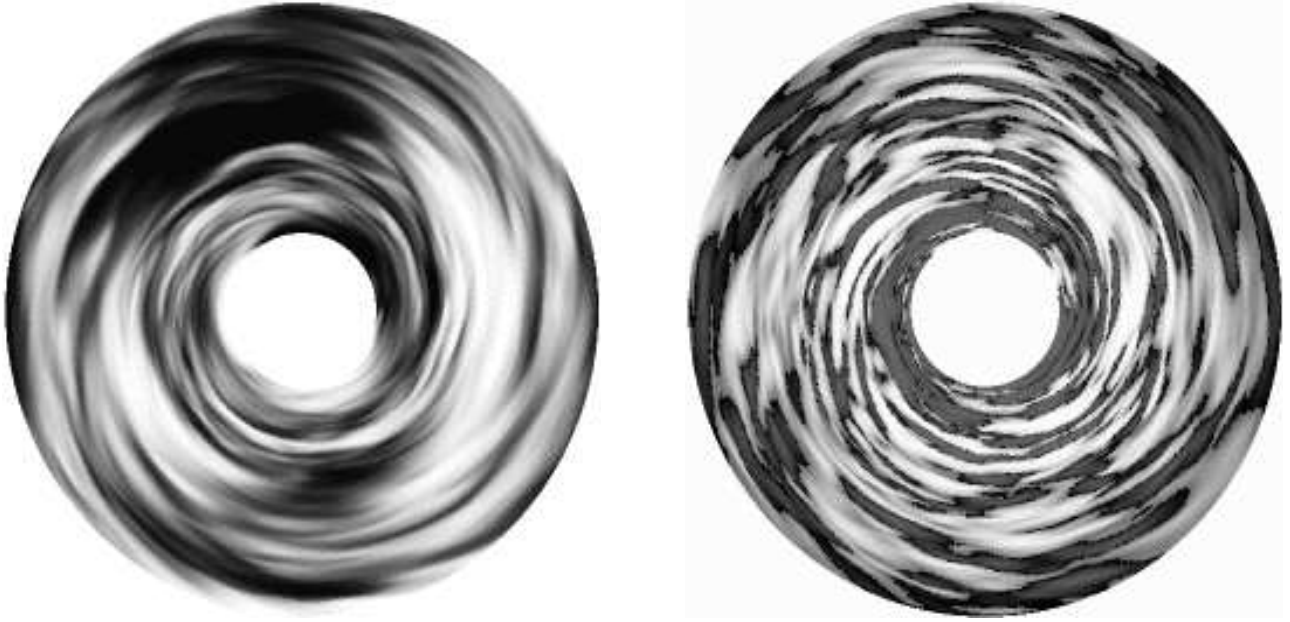


FIG. 1.— Maps of the disk surface overdensity (left image) and integrated vertical component of the magnetic field,  $B_z$  (right image), at  $t = 80$  orbits. The surface density is plotted relative to the azimuthally averaged value, ie  $\Sigma(r, \phi)/\Sigma(r)$ . Typical azimuthal fluctuations in  $\Sigma$  are at the tens of percent level, typical  $B_z$  fields are of the order of  $10^{-3}$  of the thermal energy. The disk rotates clockwise.

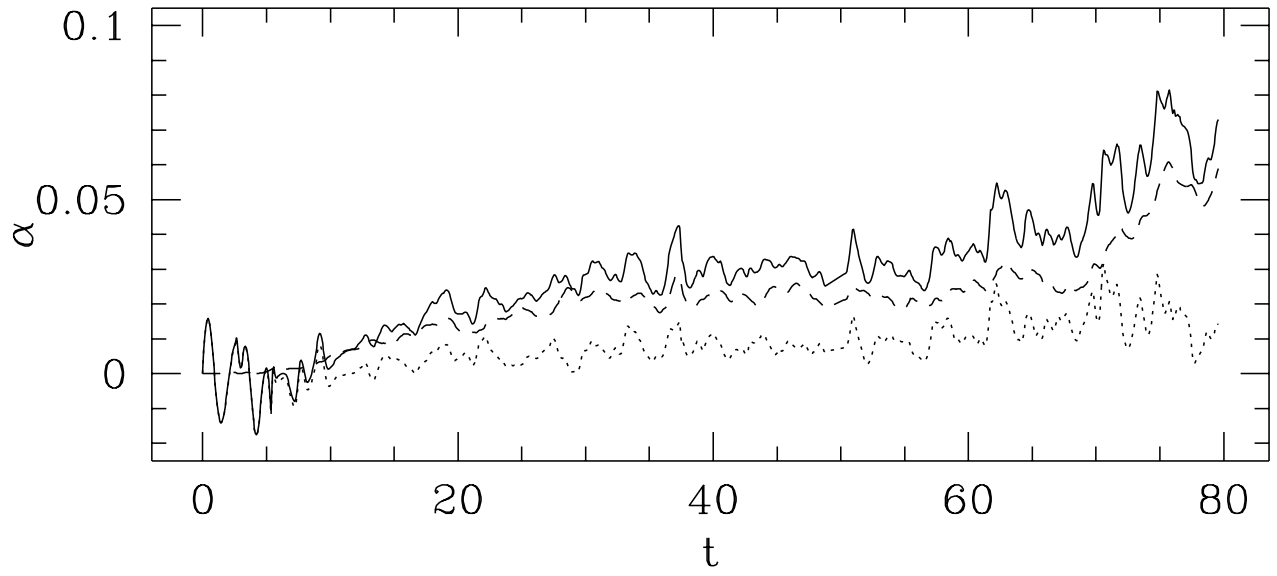


FIG. 2.— Derived Shakura-Sunyaev  $\alpha$  parameter at the center of the grid. The solid line shows the total  $\alpha$ , the dashed and dotted lines the contribution from magnetic and fluid stresses respectively.

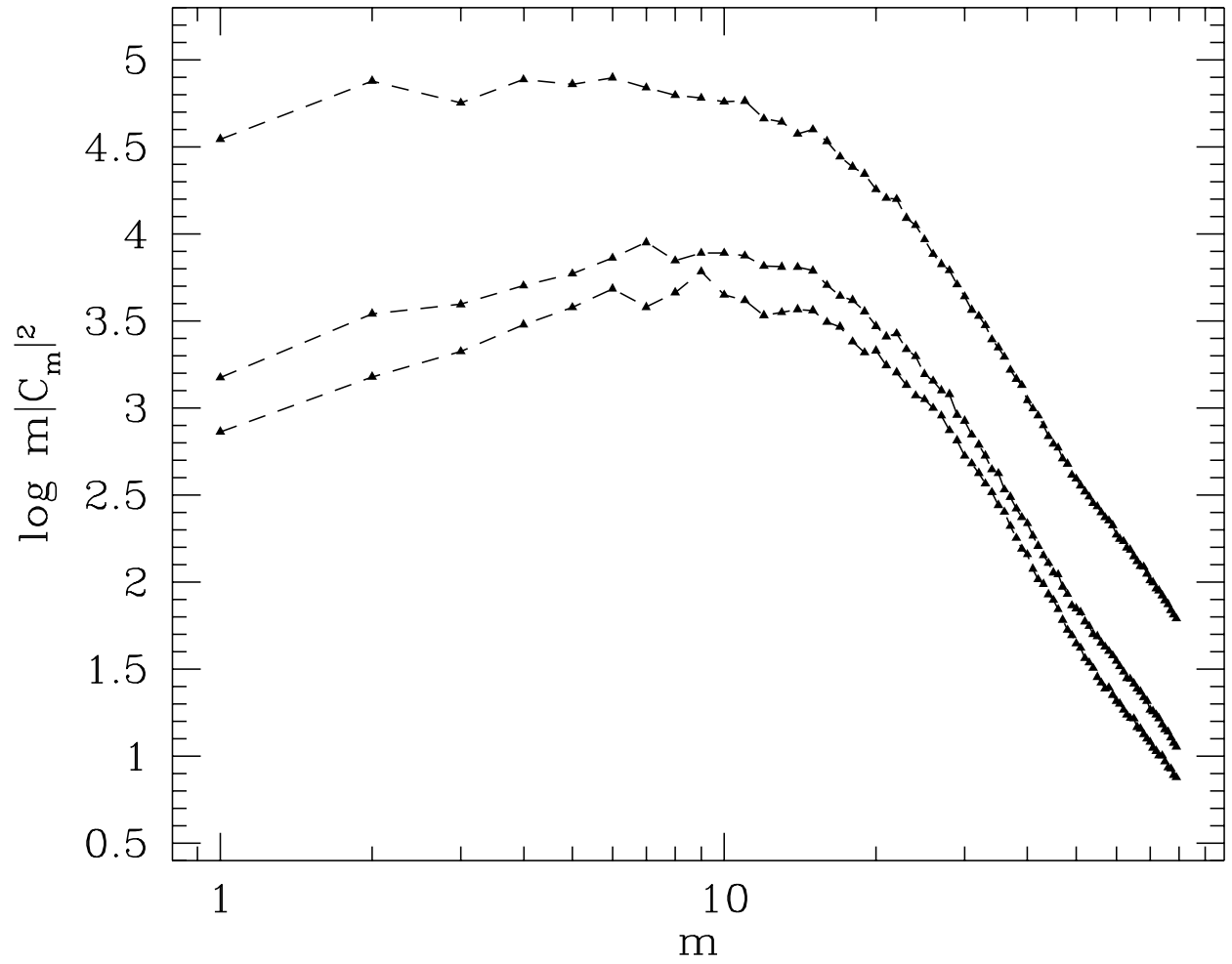


FIG. 3.— Fourier decomposition of the azimuthal structure of the disk magnetic field, averaged over the simulation volume. From top downwards, the curves show the power spectra for  $B_\phi$ ,  $B_r$  and  $B_z$  respectively.